UCRL-90807
PREPRINT

Basic and Heavy Ion Scattering in Time Dependent Hartree-Fock Theory

M. S. Weiss

Prepared for Winter School on Fundamental Nuclear Physics
ICTP, Trieste, Italy
March 11-April 13, 1984.

May 17, 1984

Lawrence Livermore National Laboratory

DISCLAIMER

Lecture I

Basics and Heavy Ion Scattering in Time Dependent Hartree Fock Theory

Prepared for Winter School on Fundemental

Nuclear Physics, Trieste, 1984 by

Morton S. Weiss

Lawrence Livermore National Laboratory
University of California
Livermore, CA 94550

Work performed under the auspices of the U.S. Department of Energy by the Lawrence Livermore National Laboratory under contract number W-7405-ENG-48.

Time Dependent Hartree-Fock theory, TDHF, is the most sophisticated, microscopic approach to nuclear dynamics yet practiced. Although, as you will see, it is far from a description of nature it does allow us to examine multiply interactive many-body systems "semi quantum mechanically" and to visualize otherwise covert processes. In two lectures I can at best adumbrate an elementary introduction of what has been in recent years a very prolific activity. I hope those of you who are intrigued by specific areas will use the informal discussions to elucidate details.

In this first lecture I will state some of the properties of the TDHF equations leaving the interested reader to one of several excellent review articles[100] for the derivations. Then with a brief nod to technique, I will describe some of the applications to the collision of heavy ions. I will then take the last quarter of this lecture to literally interpret visualize with a 15 minute color movie of a heavy ion reaction which will illustrate many of the previous points. The second lecture will be less amusing and emphasize special applications of this theory.

One of the most seductive aspects of TDHF is that it is a no free parameter theory. While this does indeed provide those of us who have practiced it with a feeling of righteousness when talking to our more macroscopic collegues with their invented bulk and surface energies and various forms of anthropromorphic dissipation, what does this mean? Clearly we haven't started from nucleon-nucleon scattering data, nor QCD and calculated heavy ion reactions. What has, of course, happended is that in some distant past we have introduced lots of free parameters; generations of sophisticated scientists have varied them to fit other phenomena and now we can ignore our disreputable origins with a "no parameter theory". TDHF is only the dynamical extension of ordinary, static, Hartree-Fock (HF) theory.

Hartree-Fock is used to study atomic nuclei through the introduction of an effective 2 body potential of which a typical example is

$$v\ (\vec{k}_1,\vec{k}_2) = t_o\ (1+x_o P_\sigma) + \frac{1}{2}\, t_1\ (k_1^2+k_2^2) + t_2\ \vec{k}_1 \cdot \vec{k}_2$$

$$+\ i\ W_o\ (\sigma_1+\sigma_2) \cdot (\vec{k}_1 x \vec{k}_2)$$

The t's and W_o and x's are free parameters invented to force HF theory to adequately mimic certain choosen properties of some specially selected nuclei. This is enormously successful! Figure 100 shows you a comparison of the cross section acquired from precise measurements of elastic electron scattering on ^{208}Pb to the theoretical quantity[101] derived from the HF density.

In static HF theory the nuclear wave function is approximated by a slater determinant of independent particle orbits which obey

$$(t + \nu)\ \varphi_\alpha = \varepsilon_\alpha \varphi_\alpha$$

The φ_α and ν are, as you know from previous lectures, found not to be independent in this approximation and the equations solved iteratively. Physically each orbit is in the potential derived from the nuclear material of all the other orbits, subject to the constrant of orthonormality imposed by the Pauli-principle.

In extending this to dynamics the same physics is retained. The wave function for the system to be evolved in time must be choosen to be a slater determinant. For a collision of a nucleus with A_1 paticles onto a nucleus with A_2 particles the systems wave function is a slater determinant of $(A_1 + A_2)$ orbitals. The equations they obey are the obvious extension of the static HF equations;

$$\frac{\partial}{\partial t} \varphi_\alpha (\vec{r},t) = (t + \nu)\ \varphi_\alpha (\vec{r},t)$$

an added complication in solving these equations is that now the ν depends implicitly upon the time because it is a function of the wave functions (or at least the density). These equations can be derived in a variety of ways, perhaps most insightfully from a variational principle

$$\frac{\delta}{\delta\varphi_\alpha(\vec{r},t)} \int_{t_1}^{tz} dt \langle\psi(\vec{r},t) \mid i \hbar \frac{\partial}{\partial t} -H \mid \psi(\vec{r},t)\rangle = 0$$

where $\psi (\vec{r},t) = \frac{1}{\sqrt{A!}} \det \varphi_\alpha (\vec{r}_i,t)$ and $\vec{r} = \vec{r}_1, \vec{r}, \ldots.\vec{r}_{A_1} + A_2$

These equations have the pleasant properties that

$$\frac{d}{dt} \langle\varphi_\alpha(\vec{r},t) \mid \varphi_\beta(\vec{r},t)\rangle = 0 \qquad \text{(a)}$$

which conserves orthonormality.

$$\frac{d}{dt} \langle\psi(\vec{r},t) \mid H \mid \psi(\vec{r},t)\rangle = 0 \qquad \text{(b)}$$

which conserves energy

$$\frac{d}{dt} \langle\psi(\vec{r}_1,t) \mid \begin{matrix}\vec{P}\\ \vec{L}\end{matrix} \mid \psi(\vec{r},t)\rangle = 0 \qquad \text{(c)}$$

where $\vec{P}$ and $\vec{L}$ are, respectively, the linear and angular momentum. These conserved quantities can be very useful tests of any numerical schemes. In addition the invariance under time reversal can also be used to test the accuracy of a proceedure.

The necessity of specifying an initial condition leads us to the last invariance, gallilean. A TDHF calculation is started by solving the static HF equations and then placing the target and projectile onto a spatial grid. The individual static solutions are then boosted in velocity and direction so as to specify the initial (relative) angular momentum and energy. Figure 101 from Flocard et al,[102] shows a deeply inelastic scattering for ^{16}O onto ^{16}O at E lab 105 MeV and an initial angular momentum of 5 $\hbar$. We can extract the scattering angle and the energy lost to internal excitation. For the same energy but an initial angular momentum of 13 $\hbar$, Fig. 102 shows a different phenomena: fusion. Although in this case the calculation was persued only to $2.8.10^{-21}$ seconds, other calculations have been carried an order of magnitude longer and the system remained fused.

The properties of this system can be summarized in Fig. 103 which show a variety of trajctories labelled by their initial conditions. Figure 104 shows the relative distance of two ^{16}O as a function of time for a nearly central collision at 32 MeV in the lab. This behaviour of a converging radius substantiates our interpretation of this type of behaviour as fusion. Our information for $^{16}O + {}^{16}O$ at E lab = 105 MeV can be summarized in Fig. 105. Here we see both scattering angle and energy lost into excitation as a function of the initial angular momentum. This can be compared to experiment by using a classical interpretation. For example the fusion cross section is

$$\sigma_{fus} \,[E \text{ lab}] = \frac{\pi\hbar^2}{\mu \, E_{lab}} \sum_{\ell<}^{\ell>} (2\ell+1)$$

where μ is the reduced mass and l>< are the lowest and highest angular momentum at which fusion starts and stops, respectively. The interpretation we make of Fig. 105 is that from central collisions (0 $\hbar$ to 13 $\hbar$) the system underwent deeply inelastic scattering, then had 0.8 barns of fusion and then more deeply inelastic scattering tapering to peripheral scattering and then plain old coulomb scattering.

If this is your first exposure to TDHF and if it is not, you really shouldn't be reading this lecture, you are appropriately horrified at the fact that there appears to be calculated fusion at 15 $\hbar$ but not at 0 $\hbar$. Much effort has been spent on this point. Figure 106 shows O^{16} onto ^{40}Ca at E lab 250 MeV and 20 $\hbar$ initial angular momentum.[(103)] It is quite clear the offending projectile punches through the target even though at intermediate times it looks as if a true compound system has been formed. Figure 107 from Ref. 104 shows the structure of the fusion cross section as a function of energy and initial angular momentum. Clearly the fall in the cross section for fusion at increasing energy is due, in this calculation, to the opening of the low l window. This is reflected in Fig. 108 which compares predicted and calculated cross section for fusion. In spite of the heroic efforts of many excellent experimenters the existence of the low l window has been neither verified nor disproved.[105]

Now all of the calculations I have shown you were performed in three dimensional coordinate space with a very simple form of the HF potential.[100] In addition one ignored both intinsic spin and charge, thus reducing the number of orbits to be propagated by a factor of 4. To study much larger nuclei some of these simplifications must be removed to make the physics believable. However, something else must happen or the calculations become intractable in terms of computer time and memory. A compromise has been made in the form of the frozen approximation.[106]

Here the complexity of the three dimensional TDHF calculation is enormously simplified by assuming the single particle orbitals can be factored into a part that depends upon the coordinates in the reaction plane and the time and a part dependings only upon the direction normal to the reaction plane and time independent.

$$\psi_i\ (\vec{r},t) = \varphi_i\ (X,Y,t)\ \chi_i\ (Z)$$

The $\chi_i(Z)$ are choosen at the beginning of the problem to be one dimensional harmonic oscillator waves functions whose oscillator parameter is adjusted to minimize the total energy of the static. HF solutions with this choice the TDHF equations become two dimensional:

$$i\hbar \frac{\partial\varphi}{\partial t} i\ [(X,Y,t)] = \left(-\frac{\hbar^2}{2m}\left(\frac{\partial^2}{\partial x2} + \frac{\partial^2}{\partial Z^2}\right) + (T_Z)_i + W_i(X,Y)\right)[\phi_i(X,Y,t)]$$

where $\quad W_i\ (X,Y) = \int dZ|X_i(Z)|^2\ W(X,Y,Z)$

$$(T_Z)_i = \frac{h^2}{2m} \int dt\ \left|\frac{d\chi i}{dZ}\right|^2$$

This reduces the time of a calculation by nearly an order of magnitude while retaining the full three dimensional kinematics. Clearly we are suppressing the possibility of energy going into this normal direction. As can be seen in Ref. 106, extensive testing of this approximation was performed both statically and dynamicaly by comparing the frozen approximation against the full three deminsional calculation. For time periods of interest and energies up to several MeV/nucleon the frozen approximation was in excellent agreement with the full calculation.

One more approximation must be discussed before we can discuss the collision of large nuclei; the filling approximation. As you know the ground states of very many nuclei are deformed. In principle we could choose a spectrum of orientations for each of our initial states. This is impossible. Instead, when we solve the static HF equations, the nucleons outside the last filled shell are forced have normalization less than one so that the last unfilled shell is uniformly occuppied. This spherizes the static HF solution. Unfortunately this alters total and relative binding energies and makes mass transfers suspect.

With these caveats, the full Skyrme III potential (without spin orbit) was used to calculate ^{86}Kr onto ^{139}La at E lab = 505 MeV[107] and Figs. 109, 110 shows the projected density for 5 $\hbar$ (fusion) and, 84 $\hbar$ (deeply inelastic scattering). Even with all of the approximations above, each impact parameter took about one hour on a Cray I computer and involved the evaluation of 146 wave functions. Table I shows the results for the 13 initial conditions studied. These were calculated with a time step of $9.0.10^{-24}$ sec on a spatial grid of 1.2 fm. The interaction time in Table I is a subjective decision on the time the compound system existed. Z_{LF} is the charge on the light fragment well after separation.

Experiments[108] have measured the fusion and deeply inelastic cross section for this system at this energy. The measured fusion cross section, 170 ± 50 m.b. is consistent with all angular momentum from 0 $\hbar$ to 66 ± 10 $\hbar$ fusing. The TDHF calculation has $60 < \ell$ fusion < 80 and is consistent with experiment.

The measured deeply inelastic scattering cross section is

$$\sigma_{exp} \text{ (d.i.)} = 1020 \pm 200 \text{ m.b}$$

and the σ_{calc} (d.i.) = 987 m.b.

Figure 111 compares experiment with inelasticity as a function of scattering angle.

Mass and charge transfers are also measured as are the distribution in mass and charge of the final fragments. Time does not permit a discussion of that type of calculation. Suffice that while the initial TDHF slater determinant is factored into its target and projectile, the final one is not. Off block diagonal terms proliferate, which means that the final fragment is not an eigenvalue of the number operator. Nevertheless the calculated distributions are much smaller than experiment, in part due to the slater det. limitation and possibly also to the "soliton nature" of the TDHF solutions (assuming they are logically separate). The inadequarcy of the calculation to get the appropriate mass transfer would be more puzzeling if we were not making the filling approximation. Because of it, the relative binding energy of both the initial nuclei and final fragments is mis-represented and it is reasonable that mass and charge flow would be incorrectly calculated.

I will conclude this lecture with a movie of the ^{86}Kr + ^{139}La calculation. I remind you that you are watching the projected density taken directly from the calculation. There is no artistic interpretation. I suggest you pay particular attention both to the properties of the neck both as to its structure and time dependence. This type of behaviour is not included in macrosopic calculations. In addition you may find the periphery or surface most intriuging. Lastly you will notice that the exterior shape is very distorted in the final fragments regardless of the level of violence in the collision whereas the interior is much more sensitive to the impact parameter.

At best this is an abbreviated menu of what has been done in this area. Many calculations with a multitude of approximations exist and if you have the dubious taste to find that interesting I hope this will provide an entry to the literature.

References

100. S. E. Koonin, Progress in Particle and Nuclear Physics, 4, 1979, D. H. Wilkinson, ed. Pergamon Press, N. Y.

J. W. Negle, Reviews of Modern Physics 54, 913, (1982).

101. J. L. Friar, J. Heisenberg and J. W. Negle, Proc. Workshop in Intermediate Energy Electromagnetic Interactions with Nuclei, MIT, 1977, A. M. Bernstein, ed.

102. H. Flocard, S. E. Koonin and M. S. Weiss, Phys. Rev. C17, 1682, (1978).

103. M. S. Weiss, private communication.

104. P. Bonche, et al., Phys. Rev. C20, 641 (1979).

105. J. Huizenga, private communication.

106. K. R. Sandhya Devi and M. R. Strayer, J. Phys. G4, K97 (1978) and Phys. Lett. 77B, 135 (1978). S. E. Koonin, et al., Phys. Lett. 77B, 13 (1978).

107. P. Bonche, et al., (no longer in preparation); results and discussion may be found in M. S. Weiss, Dynamics of H. I. Collision, N. Cindro, ed, (1981).

108. R. Vandenbosch et al., Phys. Rev. C17, 1672 (1978).

Figure Captions

Figure 100 Elastic scattering cross section of ^{208}Pb compared to that calculated from HF density. From Ref. 101.

Figure 101 ^{16}O onto ^{16}O at E lab = 105 MeV, initial angular momentum = 5 $\hbar$. The curves are isocontours of density projected onto the reaction plane. The scattering angle and inelasticity can be extracted. Fig. Ref. 102.

Figure 102 As above but for initial angular momentum = 13 $\hbar$. For obvious reasons this result is assumed to represent fusion. From Ref. 102.

Figure 103 The radius vector between centers of mass for ^{16}O onto ^{16}O at E lab = 105 MeV labelled by their initial angular momentum. From Ref. 102.

Figure 104 As above for E ebo = 32 MeV. It is this type of damping with time that makes us confident this type of event represents fusion. From Ref. 102.

Figure 105 Scattering angle and energy loss for $^{16}O + ^{16}O$ at E lab = 105 MeV as a function of initial angular momentum, Ref. 102.

Figure 106 ^{16}O onto ^{40}Ca at E lab = 250 MeV for a nearly central collision. From Ref. 103.

Figure 107 The structure in initial angular momentum of the fusion cross section for $^{16}O + ^{40}Ca$ as a function of energy. From Ref. 104.

Figure 108 Experimental and calculated fusion cross section for $^{16}O + ^{40}Ca$. From Ref. 104.

Figure 109 $^{86}Kr + {}^{139}La$ at E lab = 505 MeV for initial angular momentum 5 $\hbar$. Each color shows approx. a 10% change in projected density.

Figure 110 As above for 84 $\hbar$.

Figure 111 Experimental results for $^{86}Kr + {}^{139}La$ at E lab = 505 MeV on which are superimposed results of TDHF calculations.

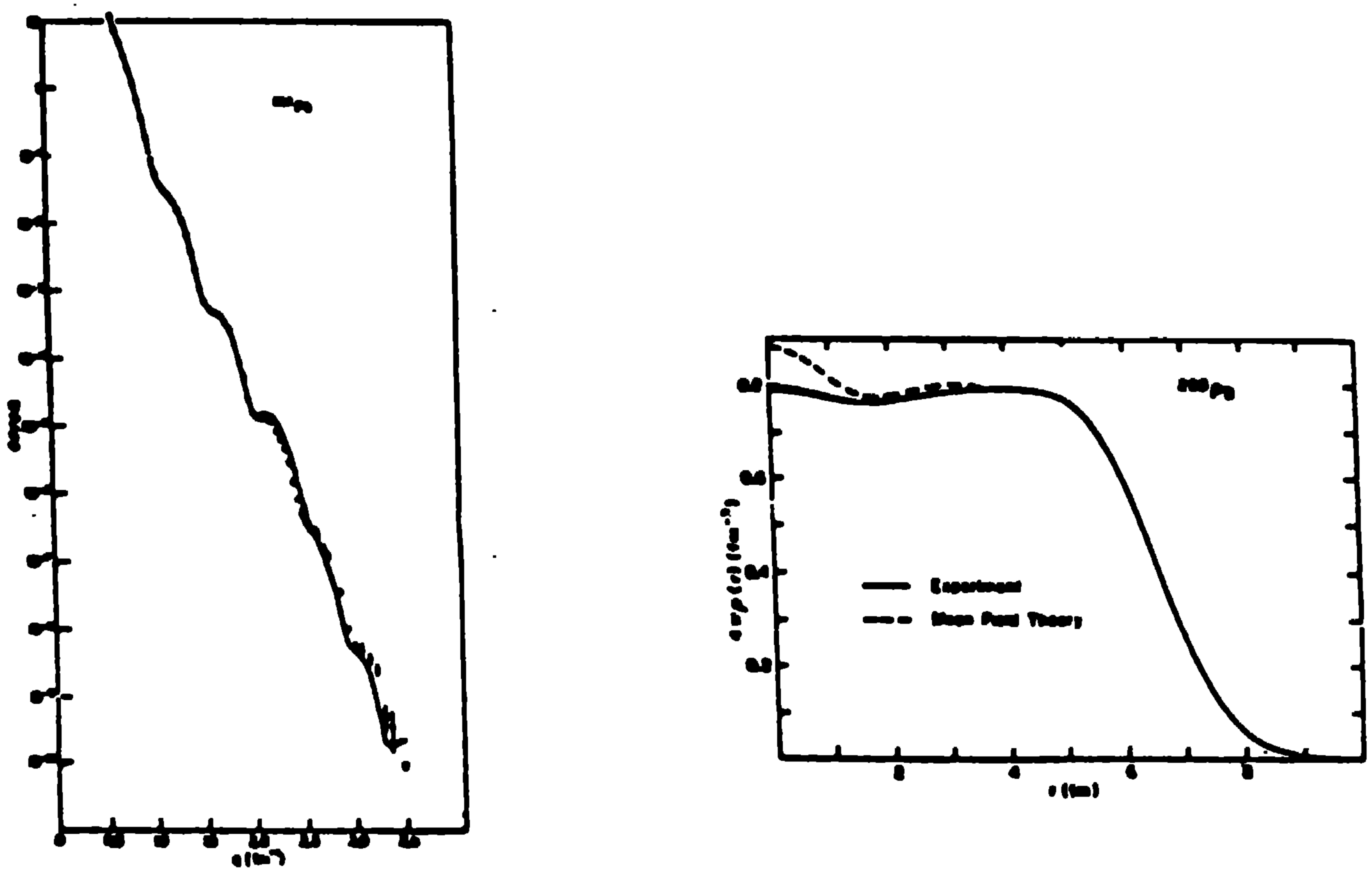

fig 100

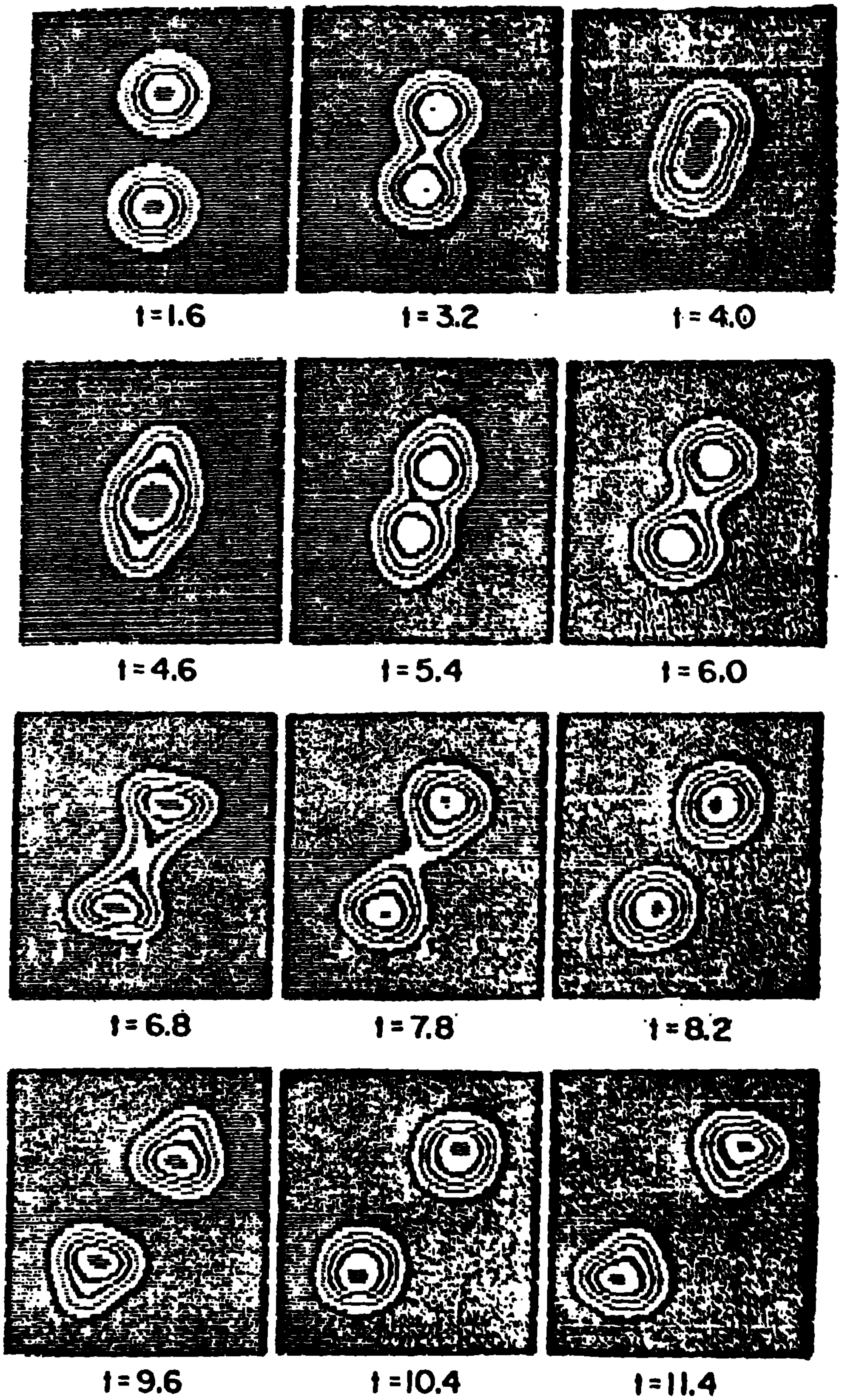

XBL 777-1530

Fig 101

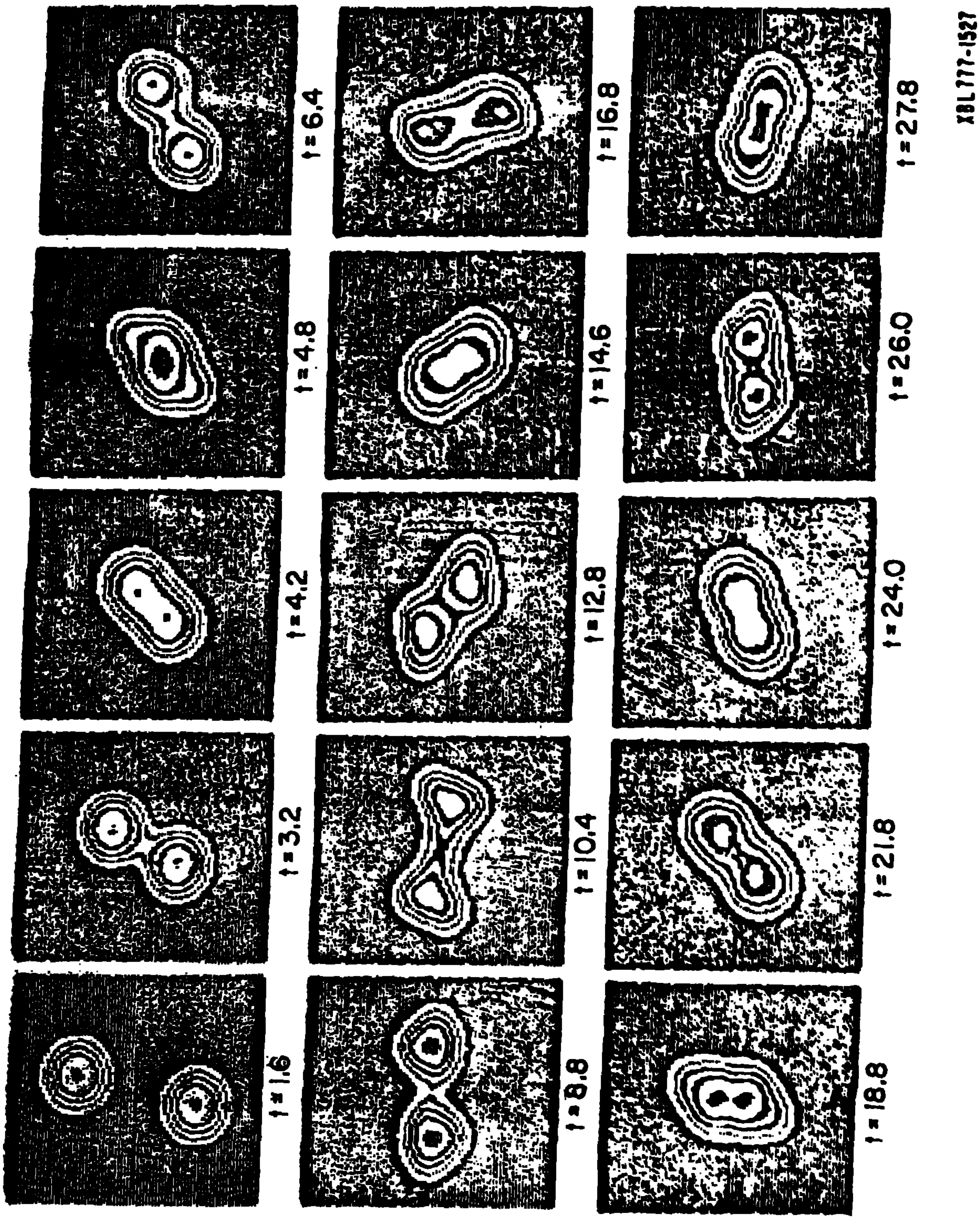
t=1.6
t=3.2
t=4.2
t=4.8
t=6.4
t=8.8
t=10.4
t=12.8
t=14.6
t=16.8
t=18.8
t=21.8
t=24.0
t=26.0
t=27.8
XBL 777-1527

Fig 102

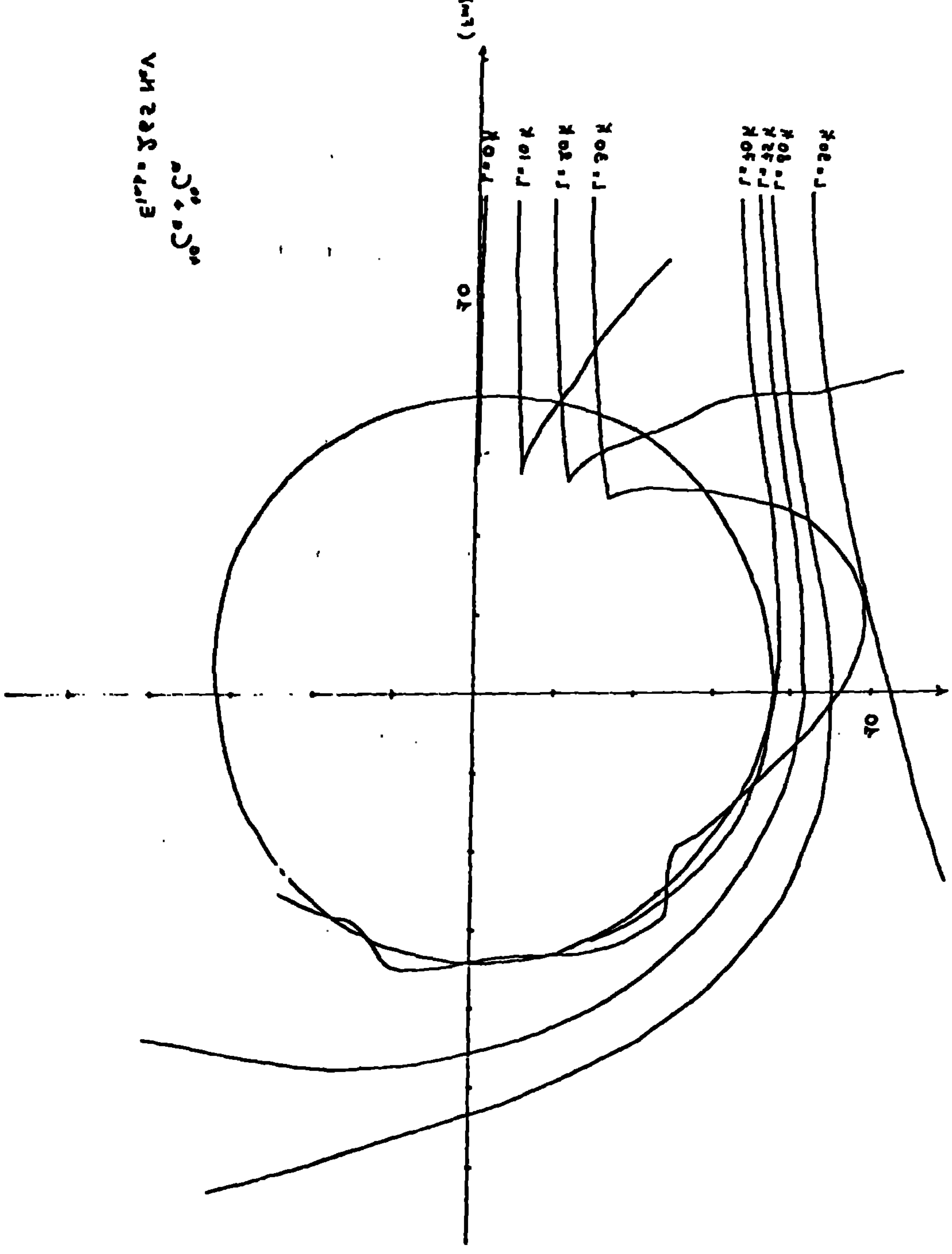

Fig 103

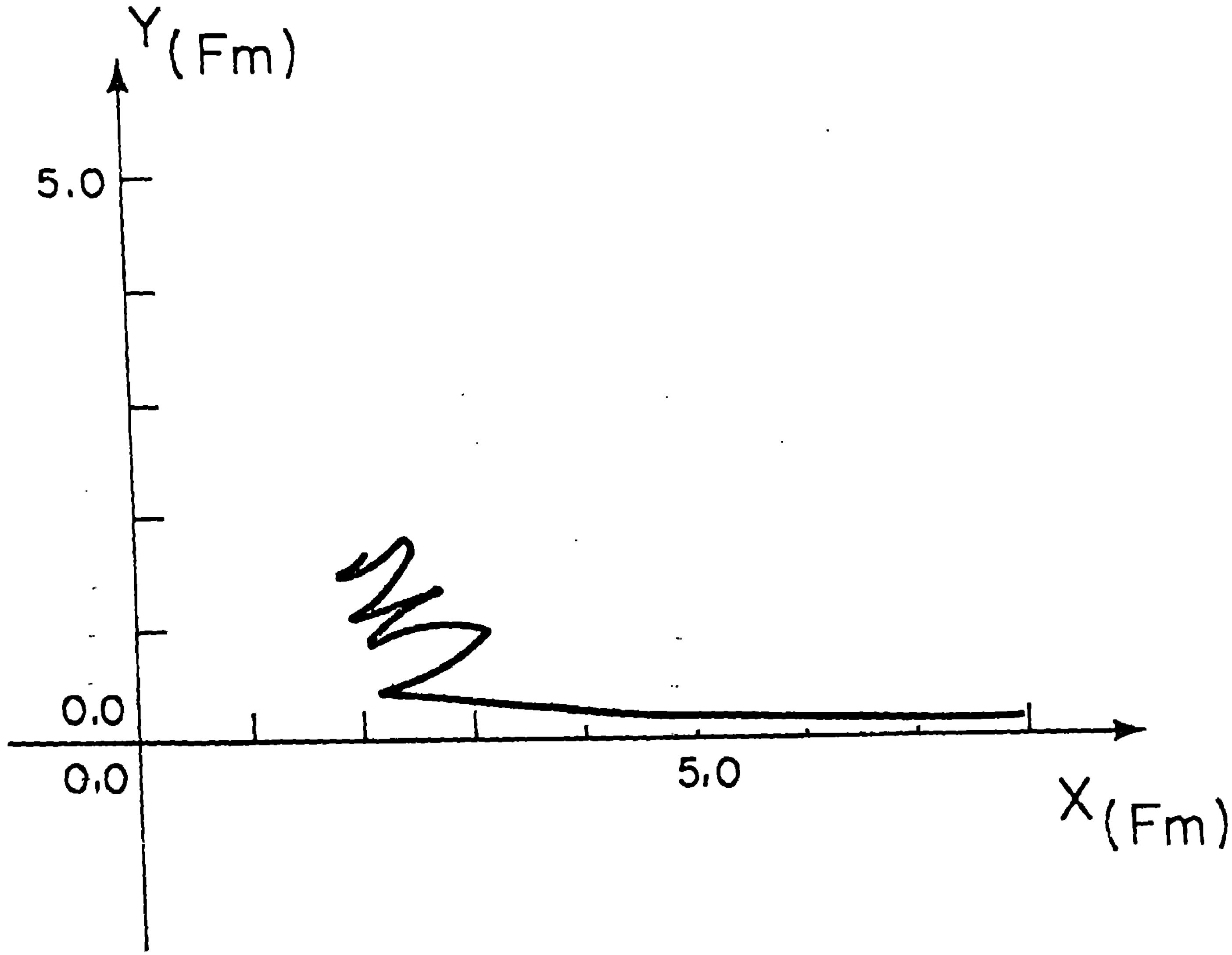

Fig 104

XBL 777-1525

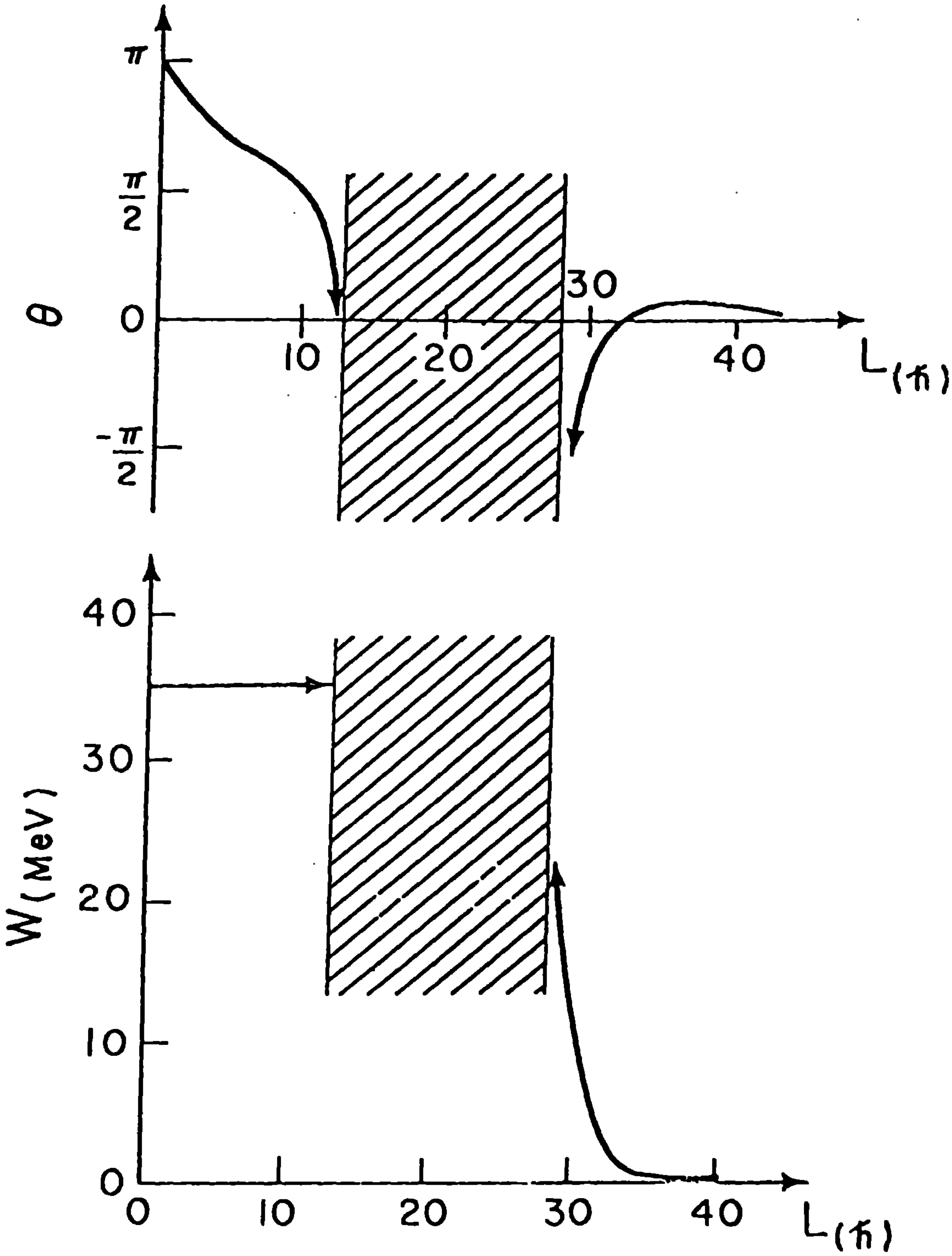

XBL 777-1524

Fig 105

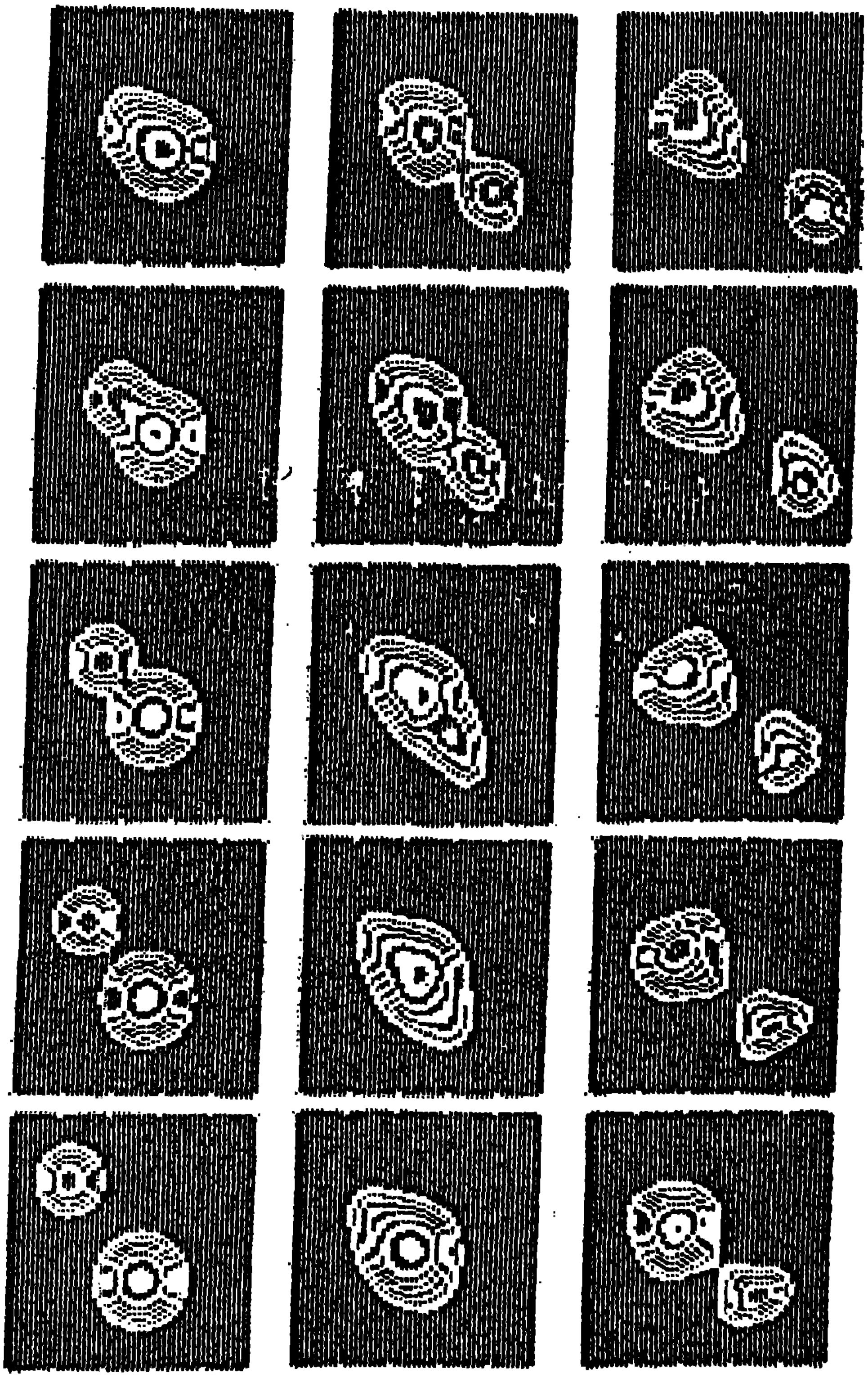

XBL 778-2952

Fig 106

Fig 107

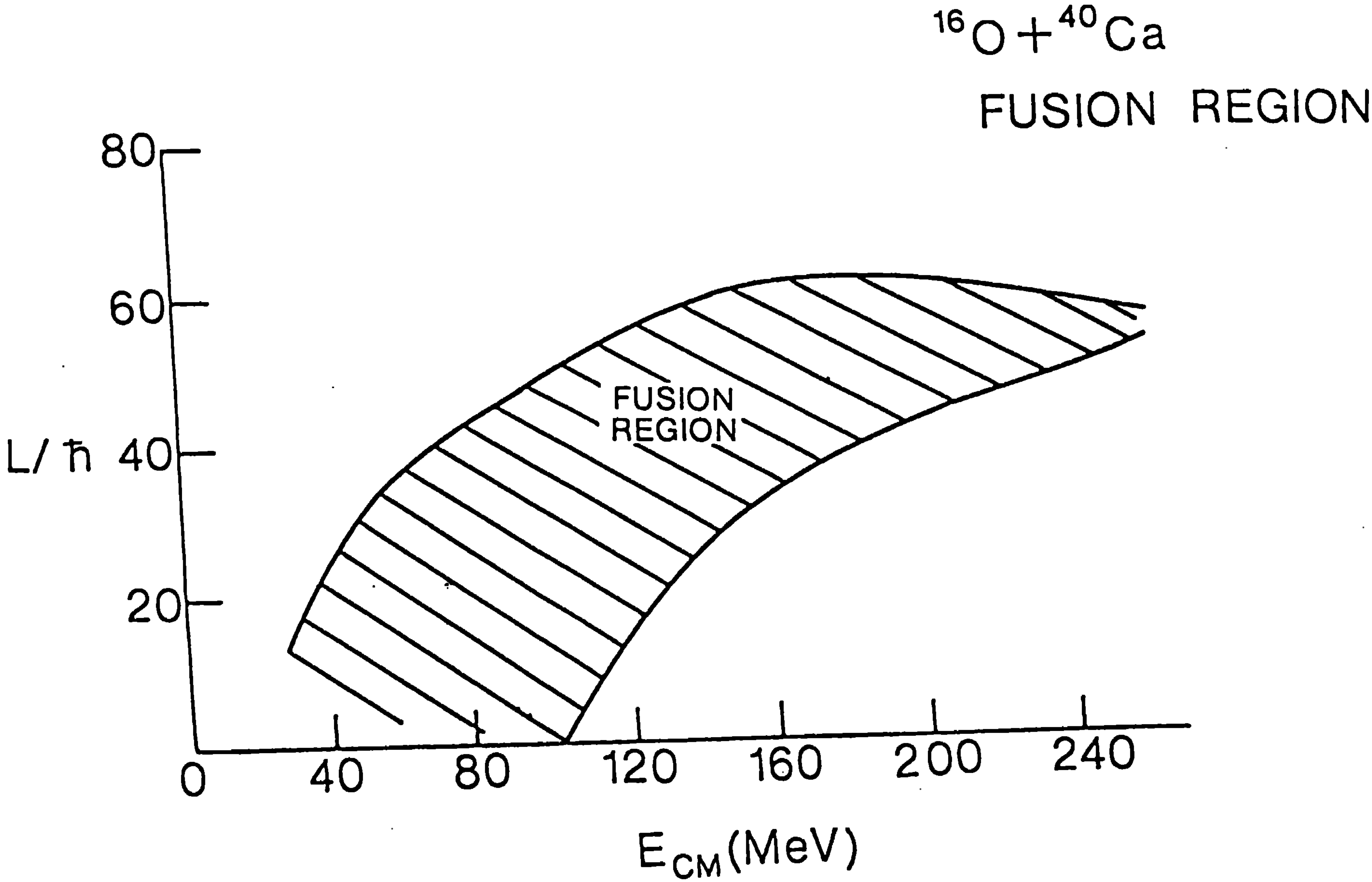

$^{16}O + ^{40}Ca$
FUSION REGION
FUSION
REGION
L/ħ
80
60
40
20
0
40
80
120
160
200
240
E_{CM}(MeV)

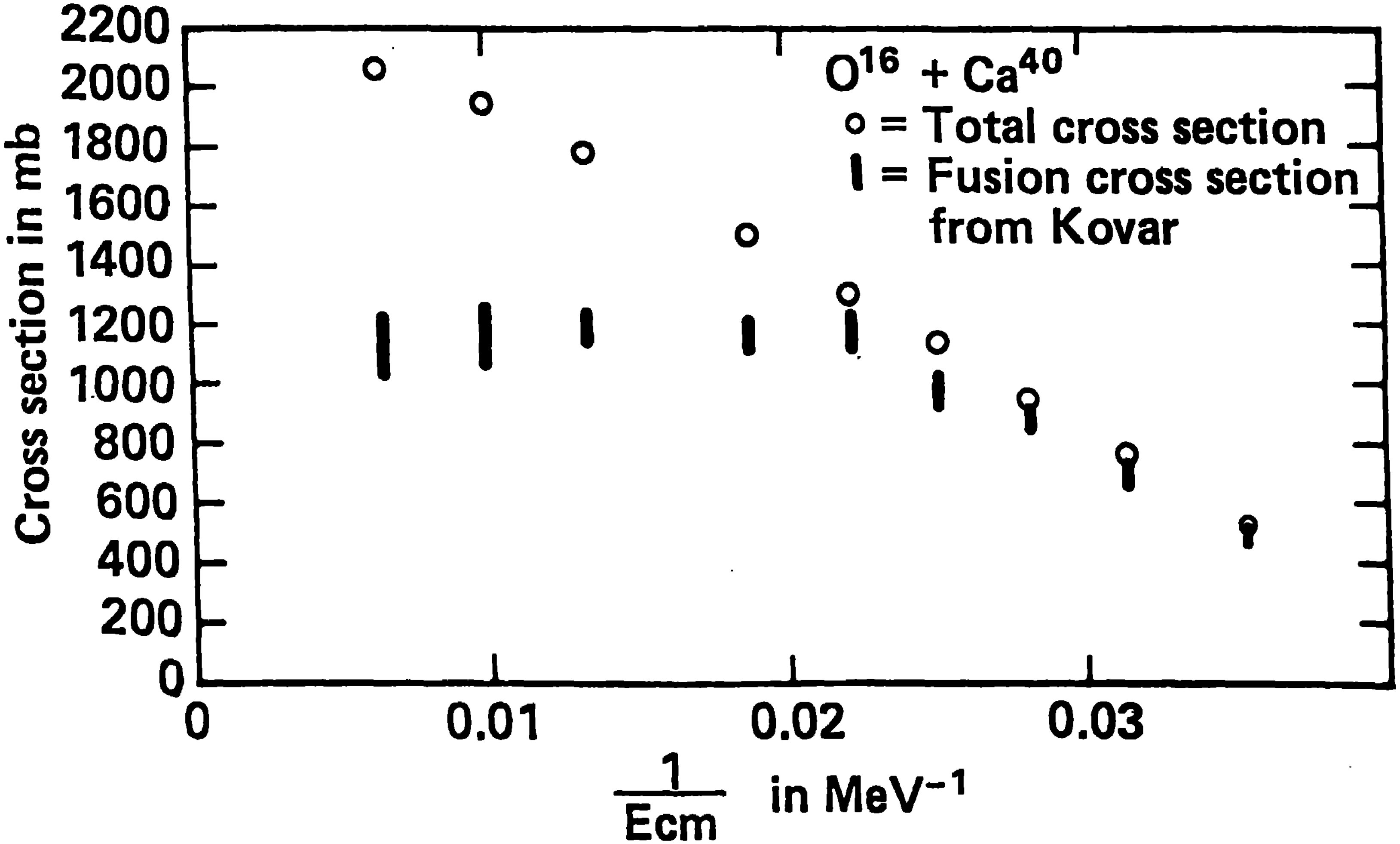
$O^{16} + Ca^{40}$
○ = Total cross section
▮ = Fusion cross section from Kovar
Cross section in mb
2200
2000
1800
1600
1400
1200
1000
800
600
400
200
0
0
0.01
0.02
0.03
$\frac{1}{Ecm}$ in MeV^{-1}

Fig 108

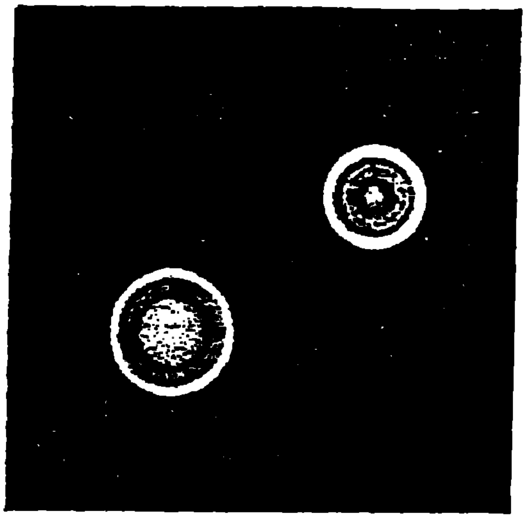

$t = 0$

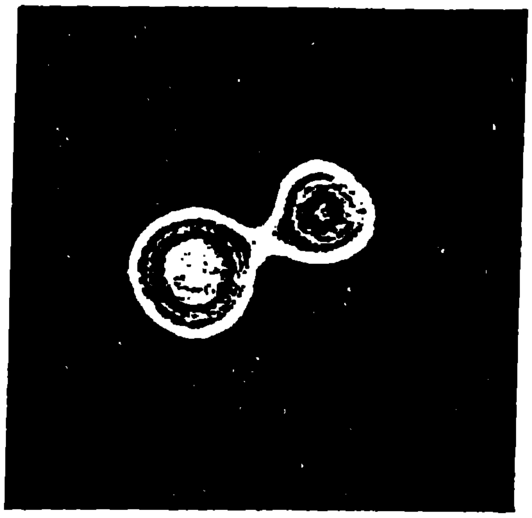

$t = 4.5 \times 10^{-22}$

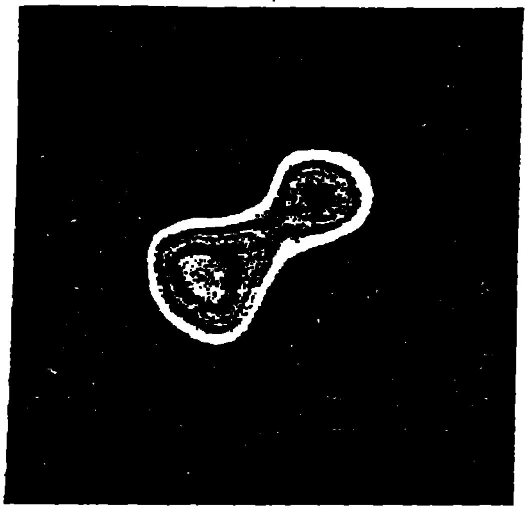

$t = 1.8$

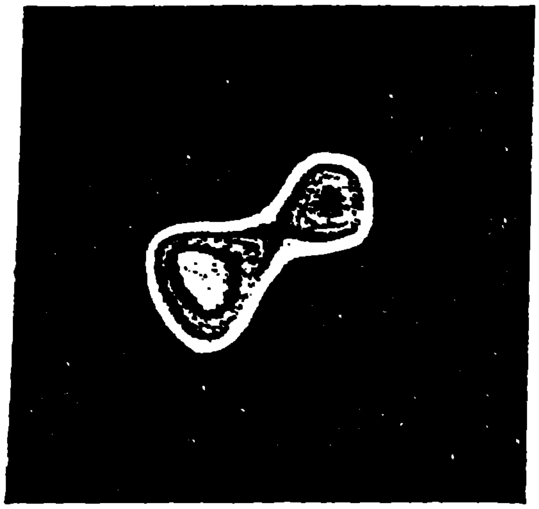

$t = 3.6$

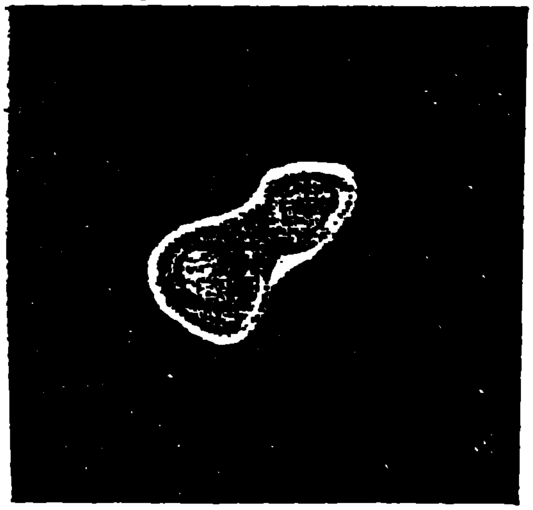

$t = 45$

Fig 109

$\ell = 84$

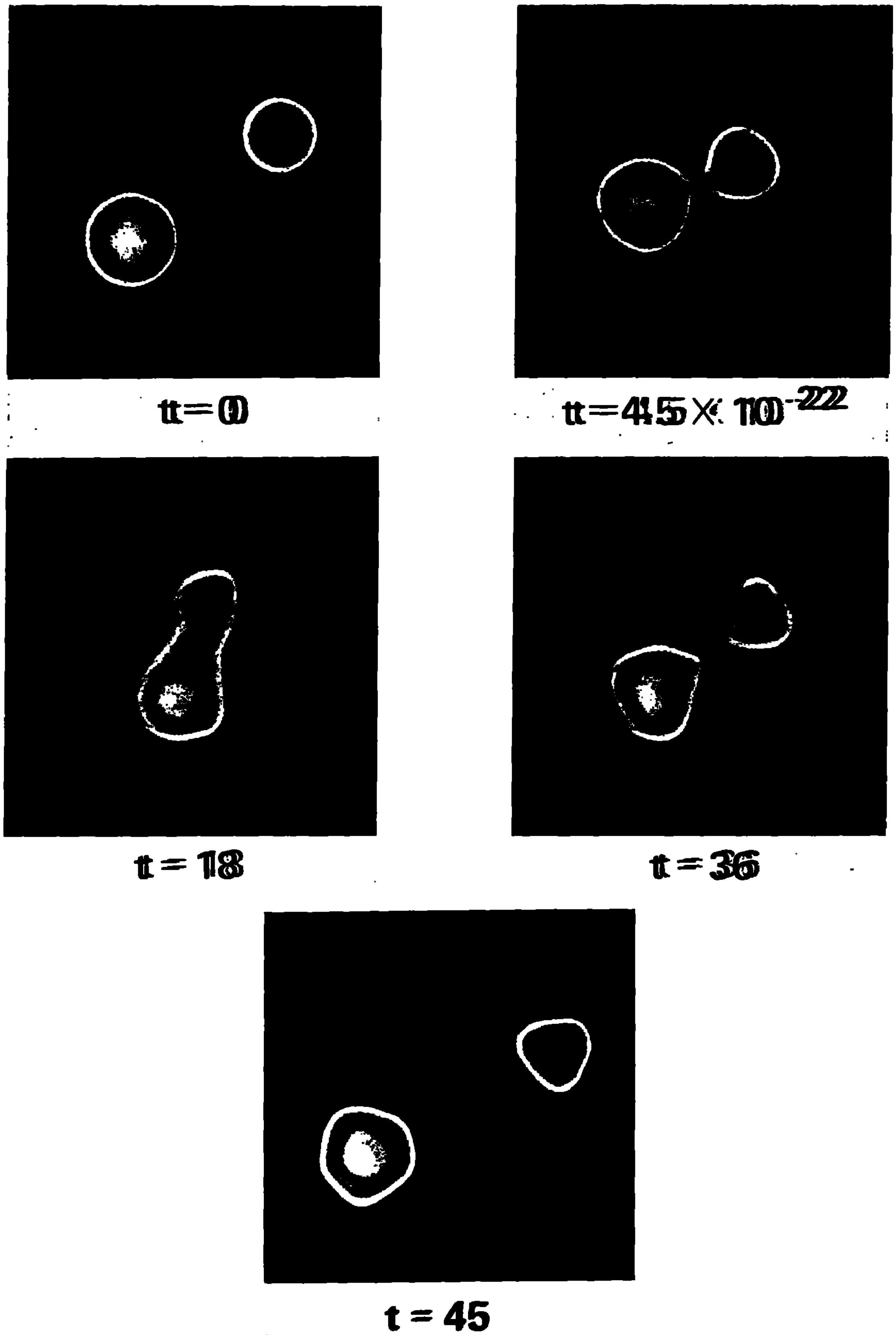

4c1110

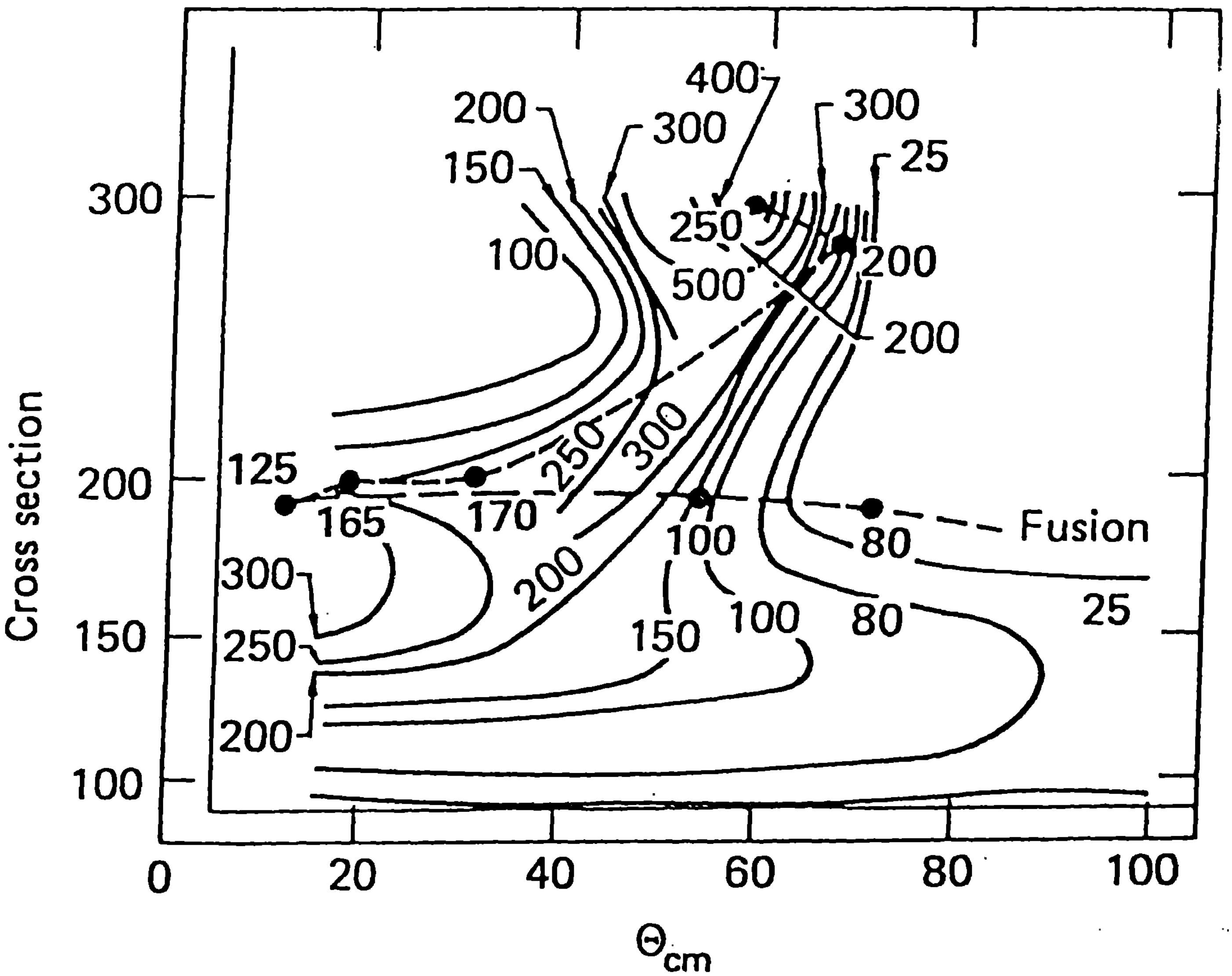
400
200
300
300
25
150
250
200
100
500
200
250
300
125
165
170
Fusion
200
100
80
300
25
150
100
80
250
150
200
100
300
200
150
100
0
20
40
60
80
100
Cross section
Θ_{cm}

Fig III